Revealing the Complex Dynamics of the Atmospheres of Red Supergiants with the Very Large Telescope Interferometer

Keiichi Ohnaka[1]
Gerd Weigelt[2]
Karl-Heinz Hofmann[2]
Dieter Schertl[2]

[1] Instituto de Astronomía, Universidad Católica del Norte, Antofagasta, Chile
[2] Max-Planck-Institut für Radioastronomie, Bonn, Germany

Massive stars lose a significant fraction of their initial mass when they evolve to red supergiants before they end their life in supernova explosions. The mass loss greatly affects their final fate. However, the mass loss from these dying supergiants is not yet understood well. Here we present our efforts to spatially resolve the dynamics of the atmospheres of red supergiants with the Very Large Telescope Interferometer (VLTI) and the AMBER instrument to clarify the physical mechanism behind the mass loss. The VLTI/AMBER's combination of milliarcsecond spatial resolution and high spectral resolution allows us to spatially resolve stellar atmospheres and extract the dynamical information at each position over the star and the atmosphere — just like observations of the Sun.

Mass loss from red supergiants

Although massive stars are short-lived and rare in number, they have a great influence on their surrounding environment. For example, powerful stellar winds and supernova (SN) explosions can trigger or quench star formation activities. They also play an important role in the enrichment of carbon, nitrogen and oxygen in the interstellar medium. Hot massive stars are also the primary source of ionising radiation in galaxies. Nevertheless, the evolution of massive stars is not yet well understood. One of the major reasons is our poor understanding of the mass loss. Particularly at the ends of their lives, massive stars experience intense mass loss. In the red supergiant (RSG) phase, the mass-loss rate dramatically increases up to ~ 10^{-4} $M_{\odot}$ yr^{-1}. Some extreme RSGs appear to have shed as much as a few solar masses.

Obviously, such drastic mass loss affects the final fate of massive stars. For example, the mass loss in the RSG phase is a key to understanding the progenitor mass of SNe Type IIP, which are the most common core-collapse SNe.

Despite its importance, the mass-loss mechanism in RSGs is one of the long-standing problems in stellar astrophysics. It is often argued that dust forms in the cool atmosphere of RSGs, and that radiation pressure on dust grains initiates a mass outflow, dragging the gas along. However, it is still controversial how and where dust forms in RSGs and there is currently no viable theory for the mass loss from RSGs. How can observations help to improve our understanding of the mass loss?

Need for high spatial and high spectral resolution

The stellar winds of RSGs are considered to be accelerated within ten stellar radii from the star, and therefore, a better understanding of the dynamics of this region — the outer atmosphere — is of paramount importance for solving the mass-loss problem. However, the outer atmosphere is very complex, as the best-studied RSG Betelgeuse (α Ori) illustrates. On the one hand, its ultraviolet image taken with the Hubble Space Telescope shows a chromosphere extending up to two to three stellar radii (Gilliland & Dupree, 1996). On the other hand, the radio map taken at 7 mm with the Very Large Array reveals cooler gas at 1000–3500 K, which also extends to about two stellar radii (Lim et al., 1998). Infrared spectroscopic and interferometric observations also suggest the presence of a molecular outer atmosphere, known as the MOLsphere, at 1000–2000 K extending to about 1.3 stellar radii (Ohnaka et al. [2011] and references therein). This means that the hot chromospheric gas (6000–8000 K) and cooler neutral and molecular gas (1000–3500 K) coexist within a few stellar radii. Perhaps the hot chromospheric gas is confined in magnetically active regions with a small filling factor and embedded in more massive cool material (Harper & Brown, 2006).

Given the complex, multicomponent nature of the outer atmosphere, it is necessary to spatially resolve this key region, in order to clarify how the RSG winds are accelerated and understand the physics behind the mass loss. However, this is easy to say but hard to do because of the angular scale of the outer atmosphere. Even the angular diameter of the closest RSG, Betelgeuse, is a mere 42.5 milliarcseconds (mas). We need milliarcsecond spatial resolution and high spectral resolution to spatially resolve the detailed structures of the outer atmosphere and extract information about its dynamics.

Velocity-resolved aperture-synthesis imaging of stellar atmospheres with VLTI/AMBER

The near-infrared VLTI instrument AMBER (Petrov et al., 2007), which combines milliarcsecond spatial resolution achieved by infrared long-baseline interferometry and high spectral resolution of up to 12 000, provides us with a unique opportunity to spatially resolve the dynamics of the outer atmosphere. We have been working on spatially resolving the velocity field in the outer atmosphere of the best-studied RSGs, Betelgeuse and Antares (α Sco), with AMBER. We focus on the CO first overtone lines near 2.3 μm. These lines are ideal for probing the properties of the upper photosphere and the outer atmosphere.

Taking advantage of AMBER's high spatial and high spectral resolution, we have carried out 1D aperture-synthesis imaging of Betelgeuse in the individual CO lines with a spatial resolution of 9.8 mas, which is more than four times smaller than the star's angular diameter (Ohnaka et al., 2011). To be precise, the reconstructed 1D images represent the 1D projection of the actual 2D images of the star obtained by squashing them onto the direction in the sky defined by the linear uv Fourier plane coverage of our observations. Figure 1 presents the 1D projection images reconstructed in the blue wing, line centre and red wing within one of the observed CO lines as well as in the continuum. As seen in the figure (top left insets), AMBER's spectral resolution allows us to not only resolve the individ-

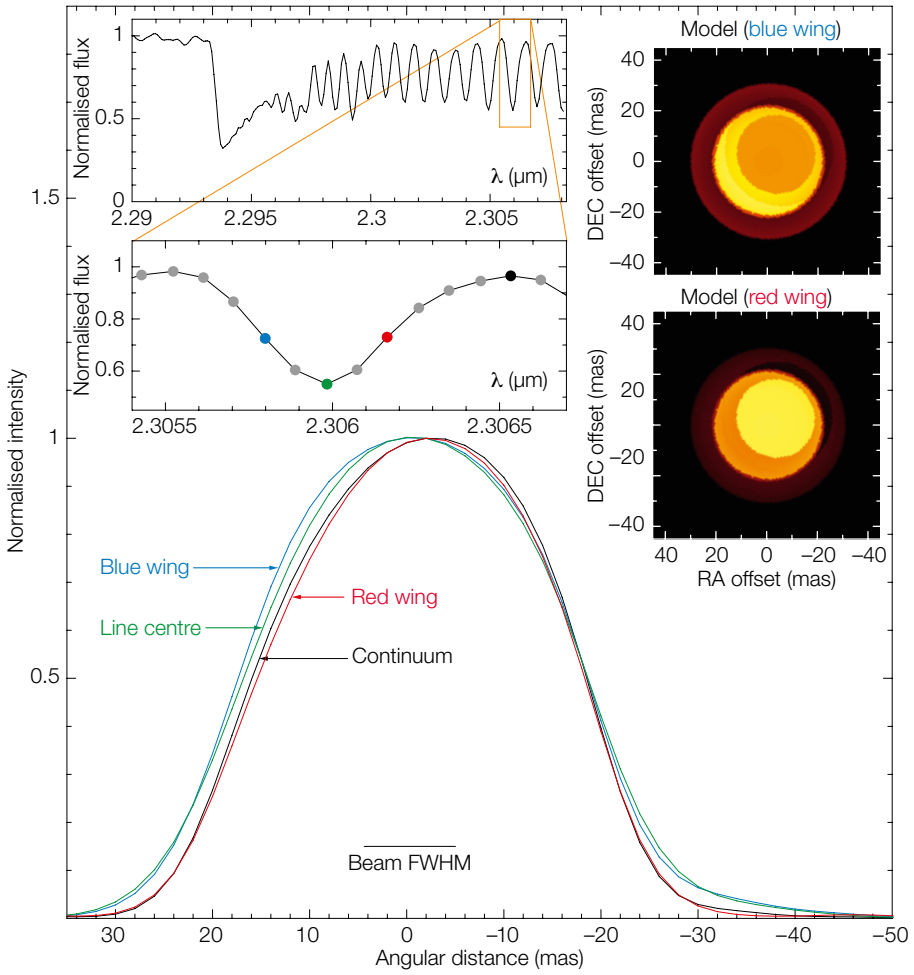

Figure 1. Velocity-resolved aperture-synthesis imaging of Betelgeuse with VLTI and AMBER. The upper left insets show the observed CO line spectrum of Betelgeuse with an expanded view of the 2.306 μm line. The 1D projection images reconstructed in the blue wing, line centre, and red wing within one of the observed CO lines as well as in the continuum are plotted at the bottom. The wavelengths of these 1D images are marked with the blue, green, red and black dots in the lower of the left insets. The 1D images are convolved with a beam of full width at half maximum (FWHM) 9.8 mas. The upper right insets present 2D images of our model in the blue and red wings of the line.

ual CO lines, but also to have approximately ten wavelength points across each CO line profile. The reconstructed 1D images in the line centre and the blue wing clearly reveal an extended atmosphere up to 1.3 stellar radii compared to the continuum image (see the profiles in Figure 1). This is the first study to image the extended, molecular outer atmosphere (MOLsphere) of an RSG in individual CO first overtone lines.

More interestingly, the star appears differently in the blue wing and red wing of the line profile. While the 1D image in the blue wing (blue line) shows the asymmetrically extended atmosphere as in the line centre, the 1D image in the red wing (red line) shows no signature of the extended atmosphere. Rather, it closely follows the continuum image (black line). This is unexpected. If the line depth is the same in the blue wing and red wing of a line, the star should appear extended by the same amount compared to the continuum. However, if the atmosphere is not static, and the velocity field is inhomogeneous (for example, the gas in some regions in the atmosphere is moving outward, while it is moving inward in other regions), the star can appear differently in the blue and red wings of the line.

We examined this idea with a simple model. The upper right insets in Figure 1 show 2D images of our model in the blue wing and red wing. We assumed a large gas clump, which is upwelling slowly at 0–5 km s^{-1}. This produces blueshifted absorption, leading to a lower intensity in the blue wing image (seen as the orange circular region in the upper right inset). On the other hand, the gas outside this clump is downfalling much faster at 20–30 km s^{-1}, which produces redshifted absorption. Therefore, as the lower right inset shows, the intensity outside the clump is lower in the red wing image (seen as the orange crescent-like shape). Obviously, the model images in the blue wing and red wing appear differently. The 1D projection images computed from these 2D model images can explain the observed change in the 1D images within the CO line profiles reasonably well. Therefore, we have spatially resolved the inhomogeneous velocity field of the outer atmosphere of Betelgeuse, which is characterised by vigorous upwelling and downdrafting motions of a gas clump as large as the radius of the star. Our velocity-resolved aperture-synthesis imaging, which is possible only with AMBER's high spectral resolution, opens an entirely new window to probe the dynamics of stellar atmospheres and winds.

Spatially resolved spectra of stellar atmospheres—observing stars as in Solar observations

The high spatial and high spectral resolution images reconstructed from the AMBER data also allow us to extract the spatially resolved spectrum at each position of the stellar disc and the atmosphere. Instead of plotting the 1D images as in Figure 1, we can make a strip of the colour-coded intensity at each wavelength. By putting these strips side by side, we obtain a 2D spectrum (Figure 2), in which the intensity is represented in colours as a function of the wavelength (horizontal axis) and the angular distance from the star (vertical axis). This is equivalent to high-resolution long-slit spectroscopy data with an angular resolution of 9.8 mas.

The 2D spectrum shows a number of spikes sticking out upward and downward at the wavelengths of the CO lines. They correspond to the extended atmosphere detected in the 1D images shown

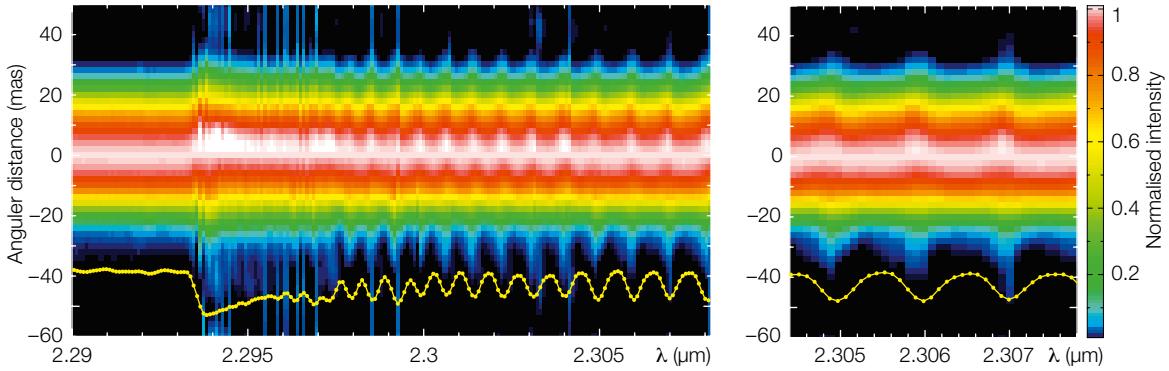

Figure 2. Spatially resolved 2D spectra of Betelgeuse reconstructed from the 1D aperture-synthesis images obtained with AMBER (left: from 2.29 to 2.308 μm; right: an enlargement for three CO lines). The spatially unresolved spectrum is shown in yellow at the bottom of both plots.

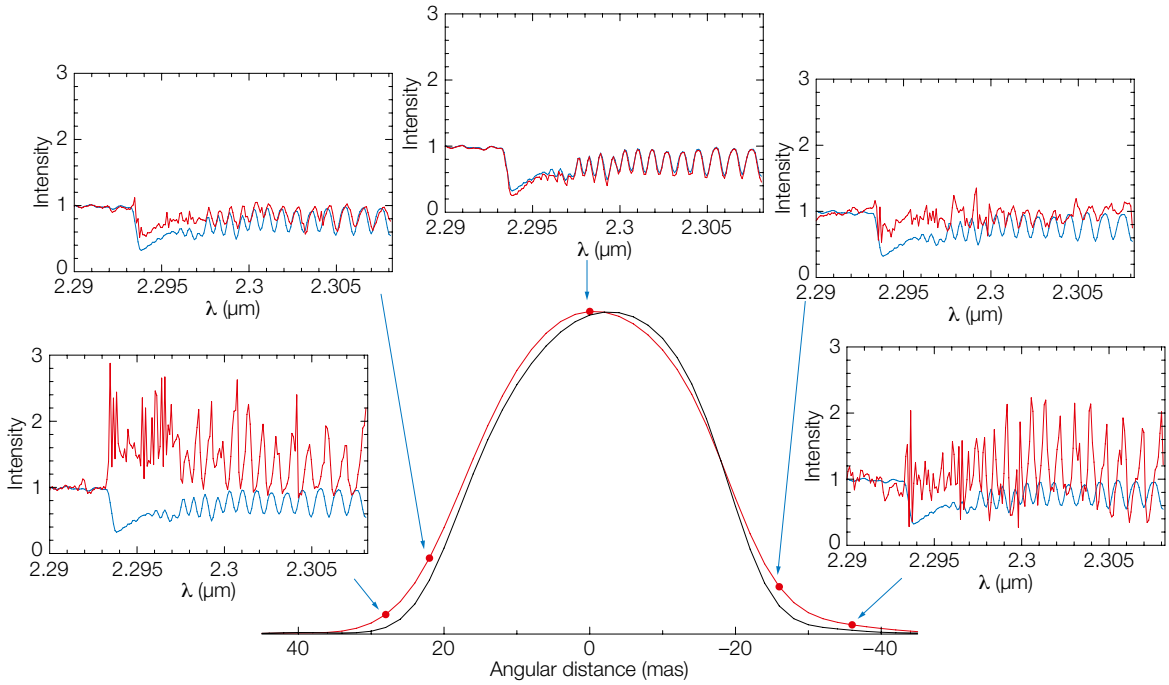

Figure 3. Spatially resolved CO line spectra of Betelgeuse extracted at five representative positions in the 1D image (red: CO line centre image, black: continuum image). In each panel, the spatially resolved spectrum is plotted in red, while the spatially unresolved spectrum is plotted in blue. All spectra are normalised to 1 in the continuum.

in Figure 1. We clearly see that the extended atmosphere is asymmetric with respect to the centre of the star: it is more extended in one direction (downward in the figure) than in the other direction (upward in the figure). The asymmetry of the extended atmosphere in the CO lines also gives rise to the wiggle running along the middle of the 2D spectrum horizontally. A closer look at the 2D spectrum, shown in Figure 2 (right), reveals that the spikes appear only in the blue half within the CO line profiles, reflecting the fact that the extended atmosphere is seen only in the blue wing and the line centre, as plotted in Figure 1.

We can extract the spatially resolved spectrum at each position by taking a horizontal cut of the 2D spectrum. Figure 3 shows the spatially resolved spectra at five representative positions derived in this manner. While the spectrum at the centre of the stellar disc (angular distance 0 mas) follows closely the spatially unresolved spectrum (that is, obtained by conventional spectroscopy), the spatially resolved spectra from the extended atmosphere (angular distances +28 and –36 mas) show prominent emission. The spectral line features become weak near the limb of the star (angular distances +22 and –26 mas), because the emission from the extended atmosphere and the absorption from the stellar disc cancel out due to the finite beam size. This result — the spectral lines turn from absorption to emission in the spatially resolved spectra of the atmosphere — is exactly what is expected from Kirchhoff's laws.

Our result demonstrates the feasibility of obtaining spatially resolved spectra over the stellar disc and atmosphere of stars other than the Sun. Moreover, it is straightforward to derive the (line-of-sight) velocity of the gas at each position and obtain a 2D map of the velocity field. We are currently working on such programmes for the RSG Antares and the red giant R Dor.

Velocity-resolved imaging of the temporally variable atmosphere of Antares

We also carried out velocity-resolved aperture-synthesis imaging of another well-studied RSG, Antares, with AMBER (Ohnaka et al., 2013). We observed in the same wavelength region with the CO

first overtone lines as in the above observations of Betelgeuse, at two epochs, one year apart. Figure 4 shows the reconstructed images across one of the observed CO lines, in which the continuum image is subtracted to enhance the extended component. As in the case of Betelgeuse, the extended atmosphere of Antares appears differently across the line profile, which means that we have spatially resolved a similar inhomogeneous velocity field in Antares as well. Moreover, while the line profiles observed at two epochs exhibit very little change (the black and red lines in the top row of the figure), the aperture-synthesis images reveal noticeable time variations. The extended atmosphere is seen in the red wing and line centre in 2009, while it is seen in the blue wing and line centre in 2010. This implies a significant change in the velocity field within one year.

What causes the vigorous, turbulent motions in the outer atmosphere?

Our velocity-resolved aperture-synthesis imaging of Betelgeuse and Antares has revealed vigorous, inhomogeneous upwelling and downdrafting motions of large gas clumps in the molecular outer atmosphere extending to at least 1.3 stellar radii. These gas motions are qualitatively similar to the motions of the much hotter chromospheric gas extending to two to three stellar radii (Lobel & Dupree, 2001). The complex gas dynamics are very different from the stationary, monotonic acceleration of the stellar winds, which is often adopted in the modelling of the circumstellar envelope.

What can be responsible for the inhomogeneous velocity field in the outer atmospheres of Betelgeuse and Antares (and perhaps RSGs in general)? The turbulent motions of large gas clumps may be reminiscent of large convective cells. However, the density of the outer atmosphere at 1.2 stellar radii derived from the observed images is ~ 10^{-14} g cm^{-3}, which is more than six orders of magnitude higher than predicted by the current 3D convection simulations for RSGs (e.g., Chiavassa et al., 2011). This suggests that while convection can induce inhomogeneities in the deep photospheric layers as observed (e.g., Montargès et al., 2014), it

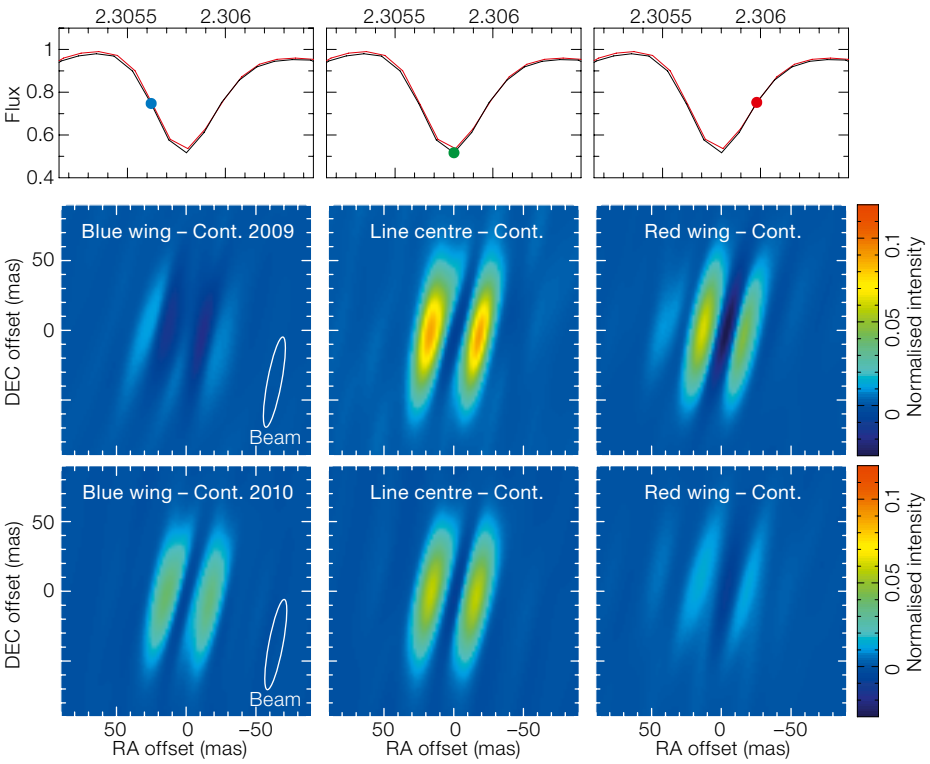

Figure 4. Continuum-subtracted aperture-synthesis images of Antares in the blue wing, line centre, and red wing (left to right) within one of the observed CO lines. The top row shows the line profiles observed in 2009 (black) and 2010 (red), with the wavelengths of the reconstructed images marked with the dots. The middle and bottom rows show the images obtained in 2009 and 2010, respectively. The beam is quite elongated because of the elongated uv plane coverage.

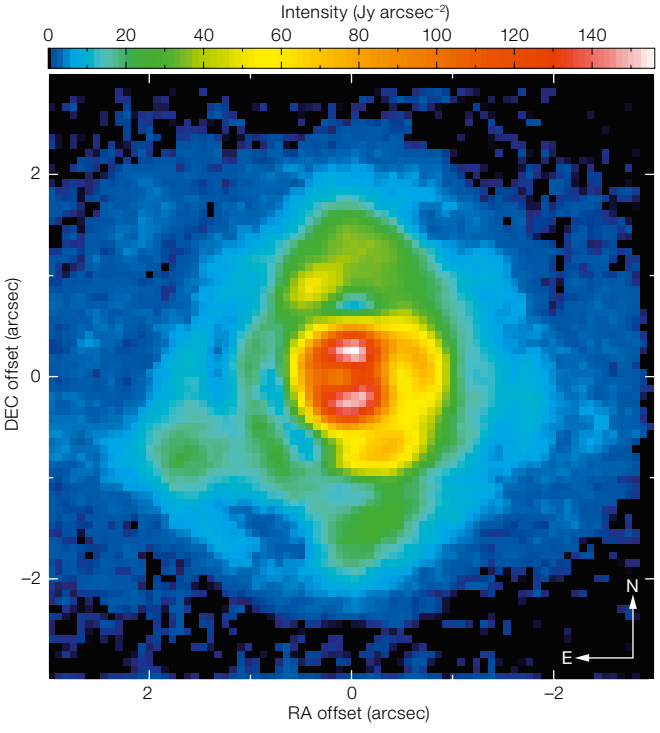

Figure 5. VISIR image of Antares obtained at 17.7 μm (Ohnaka, 2014). The central star is subtracted to clearly show the clumpy circumstellar envelope.

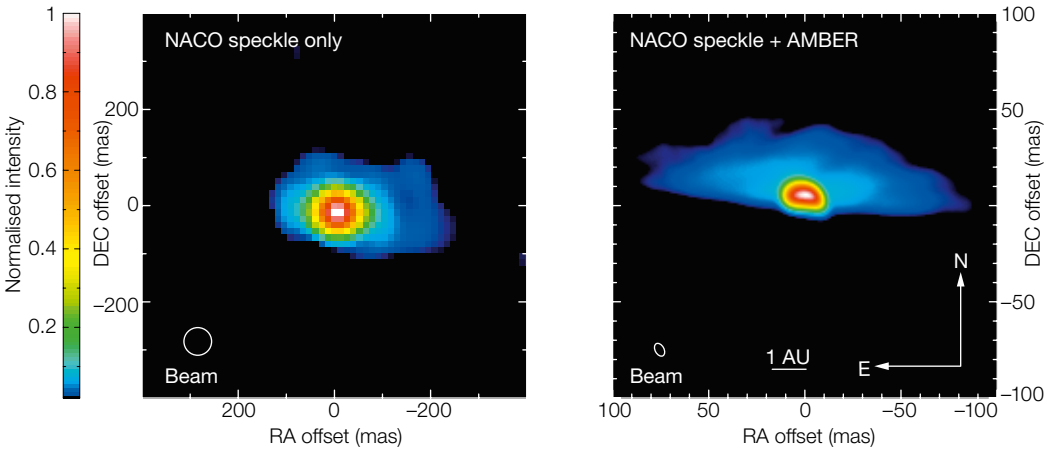

Figure 6. Aperture-synthesis imaging of the dust disc and the half-obscured central star of the red giant L_2 Pup (Ohnaka et al., 2015). Left: Image reconstructed from the speckle interferometric data obtained with NACO. Right: Image reconstructed by combining the NACO speckle data and the AMBER data.

is not sufficient to lift up the atmosphere to the observed 1.3 stellar radii.

What else can be causing the detected, inhomogeneous, vigorous gas motions? Given the detection of magnetic fields on Betelgeuse (Aurière et al., 2010), the magnetohydrodynamical (MHD) process might be responsible. However, at the moment, there is neither an observational smoking gun nor a self-consistent theoretical model to explain it. An alternative scenario is radiation pressure on molecular lines (Arroyo-Torres et al., 2015). The physical mechanism behind the vigorous turbulent motions in the outer atmosphere of RSGs remains to be unveiled.

The inhomogeneous velocity field in the outer atmosphere is likely the seed of the clumpy structures seen in the circumstellar envelope of Betelgeuse and Antares on larger spatial scales. The VLT spectrometer and imager for the mid-infrared (VISIR) imaging of Betelgeuse in the mid-infrared show an asymmetric, clumpy circumstellar envelope extending up to 2 arcseconds (or 94 stellar radii, Kervella et al., 2011). Our 17.7 µm image of Antares taken with VISIR, shown in Figure 5, also reveals clumpy dust clouds at 0.8–1.8 arcseconds, which correspond to 43–96 stellar radii. These dust clouds may have formed from large, upwelling gas clumps that were further accelerated and have managed to escape the star's gravitational potential.

Next steps

We can push velocity-resolved aperture-synthesis imaging one step further to probe the gas dynamics throughout the atmosphere. The velocity-resolved imaging in different molecular or atomic lines forming in different atmospheric layers allows us to obtain a 3D picture of the dynamics, from the deep photospheric layers to the outer atmosphere. Furthermore, the combination of this tomographic velocity-resolved aperture-synthesis imaging with the VLTI and the Atacama Large Millimeter/submillimeter Array (ALMA) observations of molecular lines will help us understand how energy and momentum propagate throughout the atmosphere to the innermost circumstellar envelope and pin down the driving force of the RSG mass loss. At the same time, we will be able to carry out imaging of the surface and atmosphere of RSGs more efficiently and for more stars with the second generation VLTI instruments GRAVITY and the Multi AperTure mid-Infrared Spectro- Scopic Experiment (MATISSE). Their accuracy and sensitivity, combined with spectral resolution of 4000–5000, will enable us to obtain detailed images of RSGs in many more spectral lines than have been explored up to now.

While the VISIR image of Antares (Figure 5) implies a link between the formation of dust clouds and the turbulent motions of large gas clumps in the outer atmosphere, we have yet to clarify where and how dust forms in RSGs. To illustrate that the imaging with VLTI is also promising for this goal, we show our recent results for the red giant L_2 Pup in Figure 6 (Ohnaka et al., 2015). We succeeded in aperture-synthesis imaging at 2.2 µm by combining speckle interferometric observations with the Nasmyth Adaptive Optics System and the high resolution near-infrared camera (NACO) on the VLT and long-baseline interferometric observations with AMBER and VLTI. The reconstructed image with a beam size of 5.6 × 7.3 mas has revealed not only the nearly edge-on dust disc, but also the half-obscured central star within the equatorial dust lane. The second generation VLTI instrument MATISSE, which will enables us to carry out aperture-synthesis imaging in the thermal infrared from 3 to 13 µm, will provide an excellent opportunity to probe the dust formation in RSGs extensively. Therefore, in the coming years, we can expect to obtain a comprehensive picture from the photosphere to the outer atmosphere to the inner circumstellar envelope, which is indispensable to finally solving the mass-loss problem.

References

Arroyo-Torres, B. et al. 2015, A&A, 575, A50
Aurière, M. et al. 2010, A&A, 516, L2
Chiavassa, A. et al. 2011, A&A, 535, A22
Gilliland, R. L. & Dupree, A. K. 1996, ApJ, 463, L29
Harper, G. M. & Brown, A. 2006, ApJ, 646, 1179
Kervella, P. et al. 2011, A&A, 531, A117
Lim, J. et al. 1998, Nature, 392, 575
Lobel, A. & Dupree, A. K. 2001, ApJ, 558, 815
Montargès, M. et al. 2014, A&A, 572, A17
Ohnaka, K. et al. 2011, A&A, 529, A163
Ohnaka, K. et al. 2013, A&A, 555, A24
Ohnaka, K. 2014, A&A, 568, A17
Ohnaka, K. et al. 2015, A&A, 581, A127
Petrov, R. G. et al. 2007, A&A, 464, 1